View metadata, citation and similar papers at core.ac.uk

brought to you by CORE

provided by Institutional Repository of the Freie Universität Berlin

Title: **Fluorescence contrast improvement by polarization shaped laser pulses for autofluorescent biomolecules**

Author(s):

B. Haas, M. B. Hild, A. Kussicke, A. Kurre, A. Lindinger

Document type: Preprint

Terms of Use: Copyright applies. A non-exclusive, non-transferable and limited right to use is granted. This document is intended solely for personal, non-commercial use.

Citation:

"B. Haas, M. B. Hild, A. Kussicke, A. Kurre, A. Lindinger, 2020, Optik, 207, 163777 ; https://doi.org/10.1016/j.ijleo.2019.163777"

Fluorescence contrast improvement by polarization shaped laser pulses for autofluorescent biomolecules

B. Haas, M. B. Hild, A. Kussicke, A. Kurre, A. Lindinger*

Institut für Experimentalphysik, Freie Universität Berlin, Arnimallee 14, D-14195 Berlin, Germany

Abstract

We present contrast enhancement for the autofluorescing coenzymes flavin adenine dinucleotide (FAD) and nicotinamide adenine dinucleotide (NADH) in glycerol using phase and polarization shaped laser pulses after the transmission through a kagome fiber. Thereto, we report a way to calculate the optimal light modulator incident polarization angle, which in general differs from the horizontal. Combining phase and polarization shaping, we can selectively excite FAD in one polarization and simultaneously NADH in the other polarization direction by third order phase functions. Due to high anisotropy, the contrast of the fluorescence depends on the polarization direction. The effect of the fiber on the phase is precompensated in order to obtain the desired phase function after the fiber. Since the relative amounts of NADH and FAD give information about cellular metabolic activity which in turn helps understand disease processes, the method promises high biophotonic potential.

Keywords: pulse shaping, optical fibers, polarization, multiphoton excitation
2010 MSC: 00-01, 99-00

1. Introduction

In recent years, multiphoton excitation of biological samples by ultrashort laser pulses became an important method for imaging [1]. Fluorescent molecules

*Corresponding author
Email address: lindin@physik.fu-berlin.de (A. Lindinger*)

were employed in order to distinguish between certain tissue structures, and a large contrast is required for microscopic imaging. This was particularly applied for investigating the metabolism of cancer cells, which is modified compared to the metabolism of non-proliferating cells in order to meet the energetic and synthetic demands of tumor genesis [2, 3, 4]. The relative amounts of the two key metabolic coenzymes, reduced nicotinamide adenine dinucleotide and oxidized flavin adenine dinucleotide, constituting the common 'redox ratio', provide a measure of cellular metabolic activity [5]. Multiphoton excited imaging of these autofluorescencing molecules is used to monitor changes in metabolism, which is an indicator of carcinogenesis [6]. This excited fluorescence method can provide diagnostic information about tumor genesis in a non-invasive manner and without the use of exogenous markers or removal of the specimen [7].

Two-photon excitation comes in handy for multiple reasons. First, the optical transition rate scales quadratically with intensity. Therefore, excitation outside the focus is suppressed, leading to reduced photo-bleaching and an increased resolution [8, 9]. Second, the tissue is exposed to infrared instead of ultraviolet photons, reducing harm due to radiation and increasing focal depths in the tissue due to reduced scattering. Third, the phase function becomes relevant and affects the multiphoton transition rate. Controlling this phase function using liquid crystal modulators builds the basis of the method in this work. Optimized phase functions can be applied that outperform even transform-limited pulses, and intensive effort has been expended on creating methods for finding optimized phase functions [10, 11]. Pulse shaping provides a powerful tool by shaping the pulses such that two species can be selectively excited [12]. Particularly, tailoring of laser pulses was conducted for multiphoton transitions, which enables exploitation of intrapulse interference effects in multiphoton excited fluorescence spectroscopy [13].

Recently, polarization pulse shaping was explored to examine the vectorial character of the light field [14, 15]. In order to perform such experiments, pulse shaping setups were assembled for simultaneous phase, amplitude, and polarization shaping, and a parametric encoding was developed [16]. With this

approach, the physically relevant parameters like chirps or polarization states can be controlled. This leads to new perspectives of modulating all properties of the light field.

In the present contribution, the phases of perpendicularly polarized subpulses are optimized by cubic phase functions for the selective excitation of FAD or NADH, respectively. These special antisymmetric phase functions will be employed for phase scans of the multiphoton excitation fluorescence [17]. Moreover, due to fluorescence anisotropy, a direction dependent contrast can be obtained which will be compared to the contrast of a flat-phase double pulse. The penetration depth for multiphoton excitation exceeds the reachable depth of a single photon process and can read up to about 1 mm into matter, as the scattering cross-section scales with ω^4. Nevertheless, multiphoton excitation is not limited to the first millimeter of tissue. Fibers can guide light to the desired location in the body. In the present study, this is simulated for endgeneous coenzymes in a liquid environment after transmitting a nanostructured fiber. A kagome fiber was chosen in this setup for its capacity for large intensities and a broad spectral bandwidth, as well as its relatively low nonlinearity and dispersion [18, 19]. Laser pulse distortions by the optical properties of the fiber can be overcome by precompensation utilizing a pulse former which facilitates receiving parametrically tailored laser pulses after the fiber [20]. Thus, the fiber enables the possibility of an endoscopic application of the method.

2. Experimental setup

Fig. 1 displays a scheme of the experimental setup. The ultrashort laser pulses are generated by a femtosecond oscillator (Mira; Coherent, Inc.) having a repetition rate of 76 MHz and a pulse energy of 5 nJ. The laser spectrum exhibits a full width at half maximum of 30 nm and a center wavelength of 800 nm. The laser pulse shaper is assembled as a zero dispersion compressor in a symmetric 4-f configuration. The laser beam is dispersed by gratings with 1200 lines/mm, and it is focused into the Fourier plane by a cylindrical lens with a 250

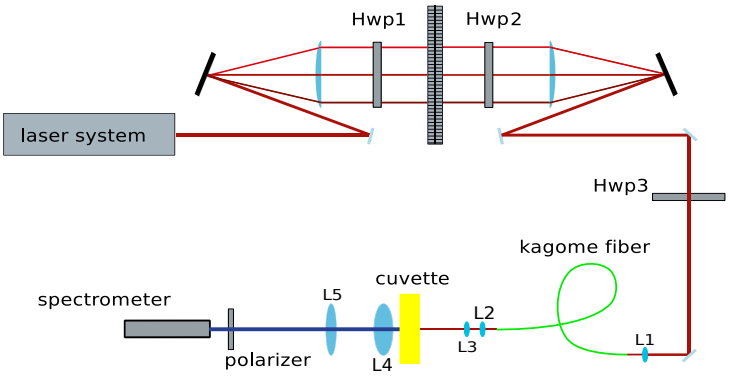

Figure 1: Experimental setup. The half-wave plates are marked by Hwp1 to Hwp3 and the lenses by L1 to L5.

mm focal length. The spatially separated frequency components are modified in the Fourier plane by a liquid crystal modulator (SLM-640, Cambridge Research Instruments) composed of two 640 element liquid crystal arrays with optical axes oriented at $\pm 45°$. The pulse shaper is able to modulate the phase and polarization independently.

After passing the pulse shaper, the laser beam is focused by a lens (L1 with f=150 mm) into a 3.4 m long kagome fiber (PMC-PL-780-USP, GLOphotonics SAS). The fiber has a 4 ring - 7 cell - hypocycloid core with a diameter of 55/70 μm, a numerical aperture of 0.009 [21], and total outer diameter of 400 μm. Behind the kagome fiber, the laser beam is collimated with lens L2 having a focal length of 300 mm. To achieve high light intensities, the shaped pulses are focused by lens L3 (f=50 mm) into a cuvette filled with FAD or NADH in glycerol. Both coencymes were received from Sigma-Aldrich Chemie GmbH and the concentrations in glycerol were 60 ± 10 mg/ml for FAD and 250 ± 30 mg/ml for NADH. The experiments were conducted at room temperature. The fluoresence signal of the coenzymes is collected by two lenses, which direct the light to a spectrometer behind an optical filter (BG 39).

3. Pulse shaping

Tailored laser pulses are guided through the kagome fiber in order to determine their optical properties. Therefore, the pulses are modulated by the pulse shaper in front of the fiber and then recorded with a two-photon diode after the fiber. The optimization algorithm, phase resolved interferometric spectral modulation (PRISM [22]), is used to receive the phase values required for a transform-limited pulse at the photodiode. The group velocity dispersion of -406 ± 20 fs^2 and the third order dispersion of 7000 ± 1100 fs^3 are calculated from the obtained settings of the modulator. Thus, it is feasible to precompensate the fiber dispersion with the laser pulse shaper, which has been conducted for the following measurements. Since the applied phase retardances are small, the possible pulse shapes after the fiber are only insignificantly confined. This allows for generating predetermined tailored pulses after the kagome fiber.

Two half-wave plates are positioned in the pulse shaper in order to modify the light polarization for compensating the polarization dependent diffraction of the second grating. The optical axis of waveplate Hwp2 located after the modulator is set to $-22.5°$ relative to the horizontal. This leads to a turn of the horizontal polarization by 45°, and the polarization components corresponding to the active axes of the liquid crystals at $\pm 45°$ are projected on the horizontal and vertical direction. This is important in order to maintain the right angle between the polarization components, modified by the active axes, even after the polarization sensitive grating and the subsequent mirrors. The first waveplate Hwp1 is used to level the intensities of the two polarization components, and Hwp3 is inserted to optionally turn the polarization. The following calculation demonstrates a way to determine the optimal polarization angle after the first waveplate, which in general differs from the horizontal due to physical properties of the involved optical elements. The optimal angle refers to equal intensities of the subpulses at the point of fluorescence for a flat phase. The electric field of the light after the second grating in time domain $\tilde{\vec{E}}^{+}_{out}(t)$ can be expressed by

$$\tilde{\vec{E}}^{+}_{out}(t) = J_{pol}\ \mathcal{F}^{-1}\left[J_{rot}(45°)\mathcal{H}(\omega)J_{rot}(\theta)\tilde{\vec{E}}^{+}_{in}(\omega)\right]. \tag{1}$$

The incident (linearly polarized) light $\tilde{\vec{E}}_{in}$ is rotated by θ at waveplate WP1. We call the effect of the manipulation due to the modulator the transfer function $\mathcal{H}$. At the second grating, the frequency components interfere. The effect of the second grating, combined with the effect of all subsequent elements, can be described as a Jones matrix of a partial polarizer plate J_{pol} with the diagonal elements p_1 and p_2 indicating the polarization sensitive reflection. The Jones vector after the second grating and the following optical elements reads:

$$\tilde{\vec{E}}_{out}(\omega) = \frac{1}{\sqrt{2}} e^{i\varphi_a} \tilde{E}^+_{in}(\omega)(\cos\theta - \sin\theta) \begin{pmatrix} p_1 \\ 0 \end{pmatrix} + \frac{1}{\sqrt{2}} e^{i\varphi_b} \tilde{E}^+_{in}(\omega)(\cos\theta + \sin\theta) \begin{pmatrix} 0 \\ p_2 \end{pmatrix} \tag{2}$$

Both polarization components are levelled for:

$$\frac{\cos(\theta) - \sin(\theta)}{\cos(\theta) + \sin(\theta)} = \frac{p_2}{p_1}. \tag{3}$$

We can rearrange equation 3 to

$$\theta = \pi n + \tan^{-1}\left(\frac{1-d}{1+d}\right), \tag{4}$$

with $n \in \mathbb{Z}$. We abbreviated $d = p_2/p_1$, implying $0 \leq d \leq 1$. For the polarization components in our experiment we obtained $d = 0.8$ which leads to an angle of about $\theta = 6.0°$, hence the half-wave plate is set to $\theta/2 = -3°$. Therefore, the waveplate can be aligned to receive the same average intensities in both polarization components. Generally, this procedure favorably includes any polarization sensitive optical element after the modulator.

In order to prevent interference between the polarization components, linear phase terms are applied on the modulator for temporally separating the two polarization components. Therefore, the phase functions can be rewritten as $\varphi_{a,b}(\omega) = \pm(\omega - \omega_0)\tau/2 + \phi_{a,b}(\omega)$, with $\phi_{a,b}(\omega)$ excluding linear phase terms. By applying the inverse Fourier transformation $\mathcal{F}^{-1}$ and taking its time shift property into account, the complex electric field in time domain after the second

grating is obtained by:

$$\tilde{\vec{E}}^{+}_{out}(t) = \frac{1}{\sqrt{2}} e^{-i\omega_0\tau/2} \tilde{E}^{+}_{a}(t+\frac{\tau}{2})(\cos\theta - \sin\theta) \begin{pmatrix} p_1 \\ 0 \end{pmatrix}$$

$$+ \frac{1}{\sqrt{2}} e^{i\omega_0\tau/2} \tilde{E}^{+}_{b}(t-\frac{\tau}{2})(\cos\theta + \sin\theta) \begin{pmatrix} 0 \\ p_2 \end{pmatrix} \quad (5)$$

with $\tilde{E}^{+}_{a,b}(t) = \mathcal{F}^{-1}[e^{i\phi_{a,b}(\omega)} \tilde{E}^{+}_{in}(\omega)]$. This yields for the two temporally separated subpulses

$$\tilde{\vec{E}}^{+}_{out}(t) = \alpha_{-} \tilde{E}^{+}_{a}(t+\frac{\tau}{2}) \begin{pmatrix} 1 \\ 0 \end{pmatrix} + \alpha_{+} \tilde{E}^{+}_{b}(t-\frac{\tau}{2}) \begin{pmatrix} 0 \\ 1 \end{pmatrix} \quad (6)$$

where we abbreviated

$$\alpha_{\pm} = \frac{1}{\sqrt{2}} (\cos(\theta) \pm \sin(\theta)) e^{\pm i\omega_0\tau/2} p_{2,1}. \quad (7)$$

Hence, the subpulses are perpendicularly polarized and temporally separated by τ. By applying further phase terms on the modulator arrays, the subpulses can be modulated individually. This is conducted by writing phase retardances on one array for one subpulse and on the other array for the perpendicular subpulse. Particularly, third order phase functions are utilized here because they have a point of antisymmetry where they reach the same two-photon signal as a transform-limited pulse, while at other frequencies they interfere destructively, which corresponds to lower intensities [13]. Therefore, a sharp two-photon signal maximum is present, which enables a selective excitation of different molecules.

4. Results

Initially, we recorded pulse shaping measurements with linear polarization for the two-photon excited fluorescence of the coenzymes FAD and NADH in order to receive the contrast and the optimal adjustments for polarization shaping. Scans of the third order phase behind the kagome fiber were conducted on the coenzymes in glycerol. Phase functions $\phi(\omega) = \frac{b_3}{6}(\omega - \omega_0)^3$ with third

order phase factor b_3 and differently tuned center frequencies ω_0 were inscribed on the modulator. Shifting of the antisymmetric phase center frequencies leads to spectrally scanned two photon maxima which allows for selective excitation of different molecules. The recorded fluorescence spectra of both coenzymes are partially seperated, which enables one to distinguish between them. FAD and NADH exhibit different slopes of the wavelength dependent absorption [1], which allows for modifying the contrast between the fluorescence emissions by phase shaping.

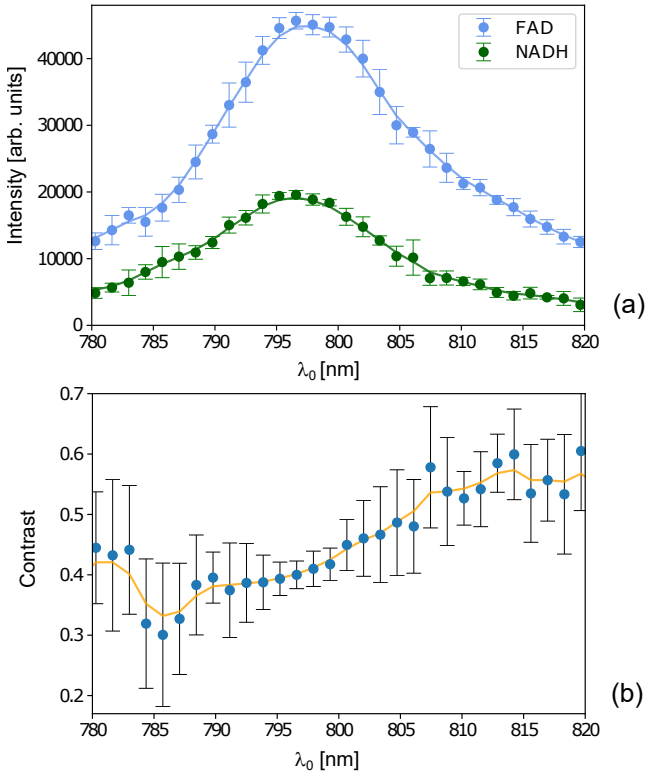

Figure 2: (a) Two-photon excited fluorescence for FAD (blue) and NADH (green) by scanning the center wavelength λ_0 of a cubic phase function with the scaling factor $b_3 = 1.0 \cdot 10^5 fs^3$. (b) Contrast between FAD and NADH showing a contrast difference of about 0.2. The measurements are averaged over 10 scans with statistical errors displayed by errors bars. The depicted lines show weighted moving averages over 2 points.

Fig. 2 (a) shows the two-photon excited fluorescence signals of FAD and NADH for linear polarization by scanning the center wavelength $\lambda_0 = 2\pi c/\omega_0$ of the cubic phase function. A wavelength shift is obtained between the received curves, since for longer wavelengths the fluorescence of FAD is higher than the one of NADH. This can be rationalized by the different slopes of the two-photon absorption. The fluorescence contrast between the two coenzymes is calculated by $(I_{FAD} - I_{NADH})/(I_{FAD} + I_{NADH})$, with I_{FAD} and I_{NADH} being the integrated fluorescence intensities. Fig. 2 (b) depicts the contrast for a scan of the central wavelength λ_0 of the third-order phase function. The measurement

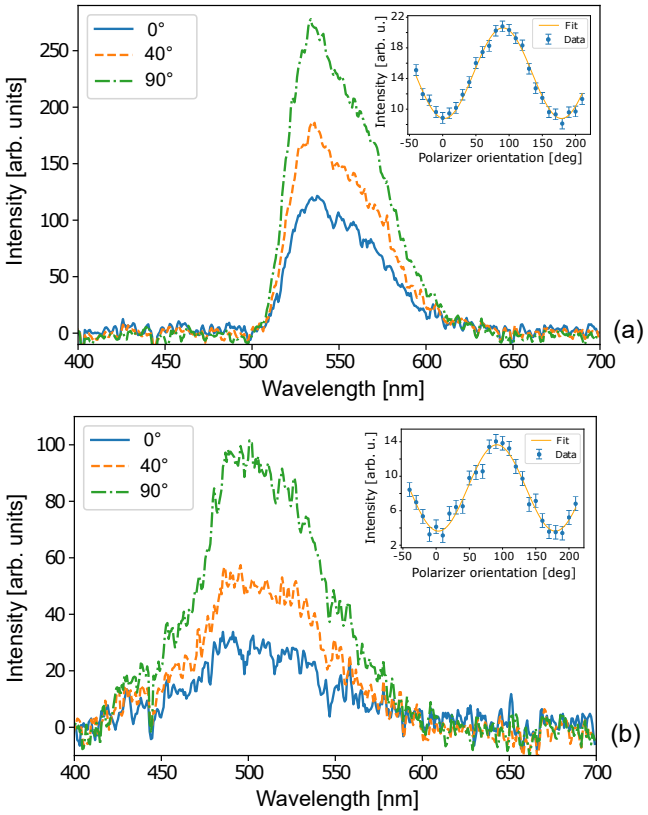

Figure 3: Polarization angle dependent two-photon fluorescence spectra of the coenzymes FAD (a) and NADH (b), respectively. The integrated polarization angle dependent signals are provided as insets. The anisotropies can be inferred to 0.31 ± 0.01 for FAD and 0.47 ± 0.03 for NADH.

shows a maximal contrast difference of about 0.2 received within the relevant spectral range from 780 nm to 820 nm. This indicates that the two coencymes can be excited separately by applying the described method.

As a next step the pulse shaping investigations are extended by additionally including polarization properties. For polarization sensitive experiments, embedding the molecules in highly viscous glycerol is required in order to keep the molecular orientation long enough until emission occurs. This leads to a fluorescence in our measurements with nearly the same polarization as the exciting light, because the coenzymes will hardly rotate away due to their considerable size, and no substantial intrinsic depolarization occurs. Thus, the fluorescence anisotropy of the excited molecules is utilized for the polarization enhanced contrast measurements. Fig. 3 presents the emission spectra of FAD and NADH for different polarizer angles relative to the horizontal, and the received angular dependent integrated signals are shown in the insets. It is noticeable that these measurements can be recorded after the kagome fiber since the polarization is well preserved after the fiber. The anisotropies in our experiment were calculated to 0.31 ± 0.01 for FAD and 0.47 ± 0.03 for NADH. These considerably high anisotropies are favorable for polarization sensitive measurements.

Finally, the optimized phase and polarization shaped laser pulse was applied, and the emission spectra after a polarizer located behind the cuvette were recorded for different polarization angles with respect to the horizontal. The specific polarization shaped pulse consists of two perpendicular phase-tailored subpulses. Thereto, the influence of the kagome fiber was compensated for each subpulse by separately applying parametric chirps, which ensures flat phases before introducing phase modulation. The chirp parameters for the subpulses were implemented by using third-order phase functions with $b_3 = 1 \cdot 10^5 fs^3$ having an antisymmetry point at 790 nm for selective excitation of NADH at one subpulse and with the antisymmetry point at 810 nm for excitation of FAD at the other subpulse. The contrasts are shown in Fig. 4 for the optimized laser pulse with two perpendicular polarized subpulses with a temporal distance of 800 fs. The results of the phase and polarization tailored pulse were compared with a pulse

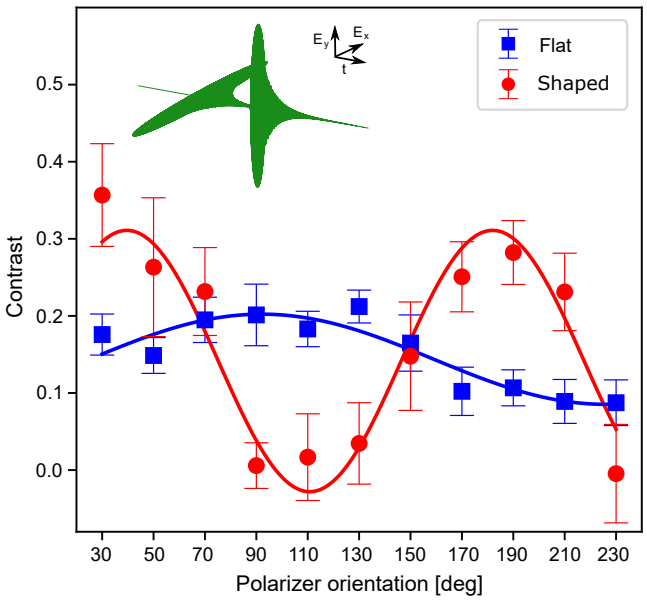

Figure 4: Fluorescence contrasts for phase shaped (red) and flat-phase (blue) double pulses as a function of the angle of the polarizer located before the spectrometer. One subpulse of the phase tailored pulse features an antisymmetry center wavelength of $\lambda_0 = 790$ nm and the other of $\lambda_0 = 810$ nm with both having a scaling factor of $b_3 = 1 \cdot 10^5 fs^3$. A distinct contrast difference is obtained for the phase shaped double pulse. The inset shows the applied simulated laser pulse.

consisting of two transform-limited perpendicular subpulses. A substantially increased contrast difference to 0.34 ± 0.03 is obtained for the phase shaped polarization components, in comparison with 0.11 ± 0.01 for the transform-limited subpulses. This phase shaped contrast difference is even larger than the corresponding value for linear polarization. The computed 3-dimensional representation of the phase and polarization shaped pulse is displayed in the inset. Thus, applying specific polarization and phase tailored pulses leads to an increased contrast difference of endogenous fluorophores, which is beneficial for imaging.

5. Conclusions

In this contribution, an increased two-photon excited fluorescence contrast of coenzymes was reported by employing predefined phase and polarization tailored laser pulses after passing a kagome fiber. The pulse modifications due to the optical fiber were precompensated to generate the desired pulseforms behind the fiber. A kagome fiber was utilized because it is favorable for novel endoscopic applications due to its unique properties with the broad transmission band and the feasibility for guiding intense laser pulses. The anisotropy of the coenzymes was determined and utilized for polarization dependent experiments with antisymmetric phase functions. A notable fluorescence intensity contrast difference was recorded between FAD and NADH by two-photon excitation with polarization shaped laser pulses. This enhanced contrast difference compared to shaping in one polarization direction demonstrates the potential of polarization shaping, because the first coenzyme is favorably excited in one polarization direction and the second coenzyme selectively in the perpendicular polarization direction. Such polarization shaped pulses allow for the investigation of the structure of tissue and they can be employed for imaging techniques. Time-dependent measurements could be helpful for biologically relevant matrices with lower viscosity, where the molecules and hence their fluorescence polarization rotate away faster. In particular, the method has a high potential for improved detection of metabolism, which is an important indication for carcinogenesis.

Acknowledgements

The Klaus Tschira Foundation (KTS) is acknowledged for funding (project 00.314.2017).

References

[1] W. R Zipfel, R. M. Williams, R. Christie, A. Y. Nikitin, B. T. Hyman and W. W. Webb, Live tissue intrinsic emission microscopy using multiphoton-

excited native fluorescence and second harmonic generation, Proc. Natl. Acad. Sci. USA **100** (2003) 7075-80.

[2] G. Kroemer and J. Pouyssegur, Tumor cell metabolism: cancers Achilles heel, Cancer Cell **13** (2008) 472-482.

[3] R. Moreno-Sanchez et al., Energy metabolism in tumor cells, FEBS Journal **274** (2007) 1393-1418.

[4] R. DeBerardinis et al., The biology of cancer: metabolic reprogramming fuels cell growth and proliferation, Cell Metabolism **7** (2008) 11-20.

[5] K. Quinn et al., Quantitative metabolic imaging using endogenous fluorescence to detect stem cell differentiation, Scientific Reports **3** (2013) 3432.

[6] S. Perry, R. Burke, and E. Brown, Two-Photon and Second Harmonic Microscopy in Clinical and Translational Cancer Research, Ann. Biomed. Eng. **40** (2012) 277.

[7] M. Skala et al., In vivo multiphoton microscopy of nadh and fad redox states, fluorescence lifetimes, and cellular morphology in precancerous epithelia, PNAS **104** (2007) 19494-19499.

[8] W. Denk, J. H. Strickler and W. W. Webb, Two-photon laser scanning fluorescence microscopy, Science **248** (1990) 73-76.

[9] G. H. Patterson and D. W. Piston, Photobleaching in two-photon excitation microscopy, Biophysical Journal **78** (2000) 2159-2160.

[10] R. S. Judson and H. Rabitz, Teaching lasers to control molecules, Phys. Rev. Lett. **68** (1992) 1500-1503.

[11] T. Brixner and G. Gerber, Quantum control of gas-phase and liquid-phase femtochemistry, ChemPhysChem **4** (2003) 418-438.

[12] A. Lindinger, C. Lupulescu, M. Plewicki, F. Vetter, S. M. Weber, A. Merli, and L. Wöste, Isotope selective ionization by optimal control using shaped femtosecond laser pulses, Phys. Rev. Lett. **93** (2004) 033001.

[13] V. V. Lozovoy, I. Pastirk, K. A. Walowicz, and M. Dantus, Multiphoton intrapulse interference. 2. Control of two- and three-photon laser induced fluorescence with shaped pulses, J. Chem. Phys. **118** (2002) 3187-3196.

[14] T. Brixner and G. Gerber, Femtosecond polarization pulse shaping, Opt. Lett. **26** (2001) 557-559.

[15] L. Polachek, D. Oron, and Y. Silberberg, Full control of the spectral polarization of ultrashort pulses, Opt. Lett. **31** (2006) 631-633.

[16] F. Weise and A. Lindinger, Full parametric pulse shaping in phase, amplitude, and polarization using an effective four array modulator, Appl. Phys. B **101** (2010) 79-91.

[17] A. Patas, G. Achazi, C. Winta, and A. Lindinger, Influence of nonlinear effects on the three-photon excitation of L-tryptophan in water using phase-shaped pulses, J. Opt. Soc. Am. B **31** (2014) 2208-2213.

[18] F. Couny, F. Benabid, and P. S. Light, Large pitch kagome-structured hollow-core photonic crystal fiber, Opt. Lett. **31** (2006) 3574-3576.

[19] M. Alharbi, T. Bradley, B. Debord, C. Fourcade-Dutin, D. Ghosh, L. Vincetti, F. Gerome, and F. Benabid, Hypocycloid-shaped hollow-core photonic crystal fiber Part II: cladding effect on confinement and bend loss, Opt. Expr. **21** (2013) 28609-28616.

[20] F. Weise, M. Pawlowska, G. Achazi, and A. Lindinger, Parametrically phase-, amplitude-, and polarization-shaped femtosecond laser pulses guided via a step-index fiber, J. Opt. Soc. Am. B **28** (2011) 406-415.

[21] PMC-PL-780-USP datasheet, received from GLOphotonics SAS.

[22] T. Wu, J. Tang, B. Hajj, and M. Cui, Phase resolved interferometric spectral modulation (PRISM) for ultrafast pulse measurement and compression, Opt. Express **19** (2011) 12961-12968.